

# Obtaining the maximum permissible gas content at the inlet to the ESP by computational fluid dynamics modeling

A Petrov<sup>1</sup> and A Sinitsyna<sup>1,2</sup>

<sup>1</sup>Bauman Moscow State Technical University

<sup>2</sup>E-mail: sin.anastasia23@gmail.com

**Abstract.** Methods for increasing the operation stability of the electrical submersible pump (ESP) are listed. Examples of computational fluid dynamics (CFD) applications for designing and studying the flow part of the pump are given. The results of mesh convergence study, Pump performance curve, and dependences of head and hydraulic efficiency on gas content at the inlet, obtained by CFD methods, are presented. The results of CFD modeling are compared with experimental curves.

## Introduction

According to statistics, in the present time, the percent of oil wells in Russia still equipped with sucker rod pumps is 34%. Installations of submersible centrifugal pumps (ESPs) account for 63% of oil wells, while 82% of oil in Russia is produced using ESPs, which indicates the effectiveness of this extraction technique [1,2]. At the same time, a significant percent of the ESP works in conditions where the petroleum contains associated gas. With high associated gas contents, reliable operation of the pumps becomes problematic, pressure and energy characteristics deteriorate, and the service life of a pump is significantly reduced. Similar results are observed during the operation of more than half of the oil wells equipped with ESP, therefore, it is necessary to learn as accurately as possible to simulate the pump operation process on a gas-liquid mixture, as well as to competently analyze the results and predict the behavior of the pump in an oil well to make further changes to the geometry of the pump flow part and for its optimization.

The problem of ESP operation on a mixture of oil and associated gas has existed for a long time, but in recent times, due to the oil wells depletion, the problem of the operation of ESPs on oil-associated gas mixture is especially topical. When gas enters the pump's flow part, gas pockets are formed, the size of which can be compared with the dimensions of the impeller channels and the pump diffuser. In this case, the energy exchange process between impeller and the liquid is frustrated, the bubbles condense, and the pressure inside the bubbles remains constant and equal to the saturated vapor pressure. The pressure of the liquid increases as the bubbles move along the channel; therefore, the pressure differential between the liquid and the pressure inside the bubble increases. With complete condensation of the bubble, a collision of fluid particles occurs, accompanied by a simultaneous local increase in pressure, reaching hundreds of MPa. This leads to the destruction of the pump working surface, the stability of its operation is frustrated, pump performance curve degradation and, as a result, a significant reduction of service life of ESP installation. To increase the stability, service life and efficiency of the ESP, the following methods are used:

1. Application of a gas disperser

It is installed at the inlet to the pump and is designed to disperse gas bubbles.



## 2. Application of a gas separator

It is installed at the inlet to the pump and is designed to separate the gas-liquid mixture into liquid and gas and to remove the separated gas into the annular space of the oil well.

## 3. Application of a gas separator-disperser (compression-dispersing modules)

It is installed instead of a gas separator or disperser in oil wells with a particularly high content of gas, where neither a gas separator nor a disperser ensures stable operation of the ESP installation.

## 4. The use of multiphase pumps stably working in gas-saturated environments.

Multiphase pumps are capable to pump multiphase liquids without separating and / or dispersing modules at the inlet, which allow them to adapt to changing oil extraction conditions.

To increase the stability of the ESP installation operation, other methods describing in detail in [3–5] are also used.

However, it is not always necessary to use one of the above methods to maintain or increase the stability of the pump - with a certain permissible gas content, the pump continues to operate stably and there is no need to use additional modules at the pump inlet, which significantly saves the financial costs of purchasing the ESP installation and reduces its dimensions. Thus, it is very important to know critical or “permissible” gas content for the designing a flow part of the pump, its optimization, the arrangement of the ESP installation and the calculation of production economic performances. It is also necessary to know the operating conditions, operation modes of pump and permissible percentage of gas as accurately as possible in order to improve the design of the flow part, the pump performance curve and increase the service life of installation.

Obtaining gas content at which the pump starvation occurs on a test bench is not a trivial task and causes a number of problems: the need to develop a test bench, and, as a result, the financial costs of its design and manufacture. In addition, significant amount of time is spent on the design and manufacture of the test bench and the manufacture of the flow part of the pump stage under test. Therefore, for obtaining permissible gas content the computational fluid dynamics method was chosen.

## Method

Today the computational fluid dynamics method for modeling flows in CFD software packages is widely used for designing the flow part, calculation the required parameters, for optimization and conducting various researches. CFD methods allow the engineer to significantly save time on calculation, optimization the parameters of the pump flow part, helping to improve the pressure and energy characteristics in the shortest possible time, as well as significantly save financial costs. There are a significant number of software packages for CFD modeling: ANSYS, STAR CCM +, FlowVision, and others. Examples of using the CFD packages for optimization the flow part of pumps and conducting a research are given in [6–11].

For computational fluid dynamics modeling, the STAR CCM + software package was chosen. The flow part of explored submersible pump for obtaining “permissible” gas content was designed in the CF Turbo software package. The flow part contains impeller and diffuser. The designed flow part and the 3-D stage model are shown in Fig. 1, 2, respectively.

### *Calculation parameters:*

- The pumping fluid is water, the recalculation of the flow part parameters and the characteristics of the pump for oil will be carried out according to fundamental work of D.Ya. Sukhanov other existing methods [12].

- $H$  (Head) = 4.9 m;

- $Q$  (Flow) = 400 m<sup>3</sup> / day = 16, 67 m<sup>3</sup> / h;

- $n$  (rotational speed) = 2900 rpm.

Using the STAR CCM + software package, the performance curve of the explored pump stage at 0% gas content was obtained, shown in Fig. 3.

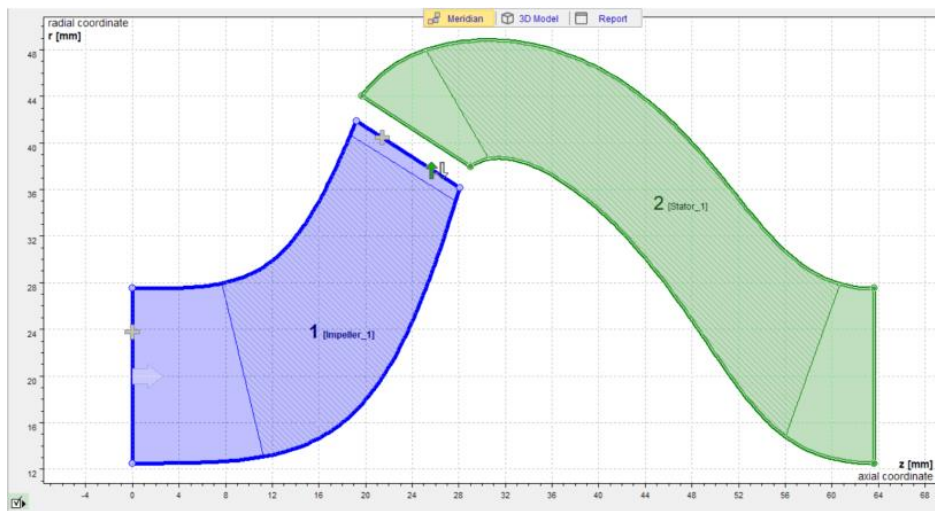


Fig. 1. Explored flow part designed in CF Turbo software package

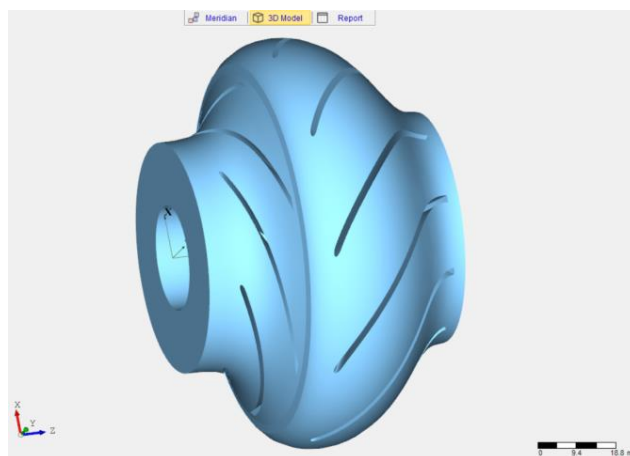
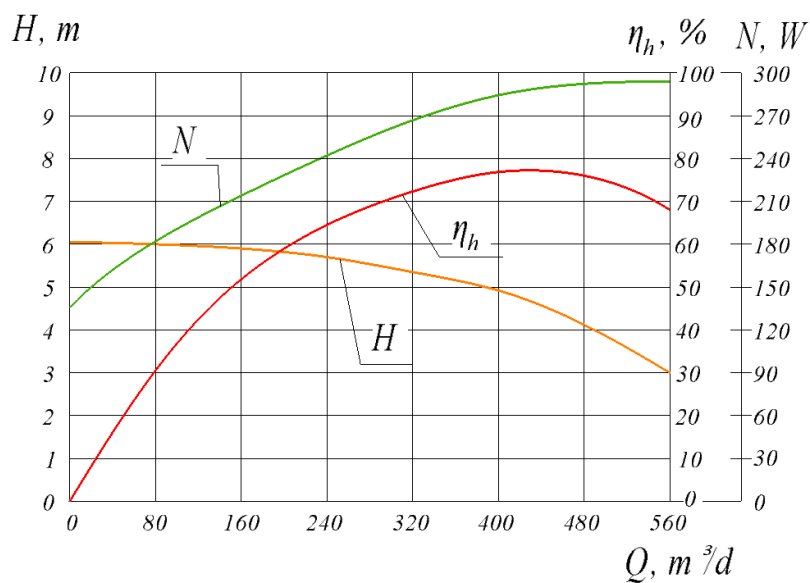


Fig. 2. 3-D model of explored flow part



**Fig.3.** Performance curve, obtained using STAR CCM+ software package

To select the optimal base mesh size, a mesh convergence study was conducted: the head value was determined at 3 values of the base mesh size: 2 mm, 5 mm and 7 mm. The time step was chosen equal to  $5 \cdot 10^{-5}$  s; accordingly,  $\approx 2000$  iterations per 1 impeller rotation. The modeling was conducted at 0% gas,  $\approx 6000$  iterations were performed for each calculation - 3 full rotations of the impeller. The most accurate result (the one closest to the previously calculated one for performance curve) and the best convergence were expectedly achieved with a mesh base size of 2 mm — the error of calculated value was less than 0.5%, however, the calculation time increases by more than 2 times in comparison with the calculation for mesh with a base size of 5 mm. The calculation of the head on a mesh with a base size of 7 mm the error is about 4%. The error in calculation the head with a base mesh size of 5 mm is about 1%; the time of one calculation is acceptable for further obtaining of dependences of head and hydraulic efficiency on gas content at the inlet. Moreover, to accelerate the calculation, only the H values were compared, assuming that hydraulic efficiency would have approximately the same error. The results of mesh convergence study are shown in Table 1:

**Table 1.** The results of mesh convergence study

Base size, mm	Number of cells	Time of calculation, min	H, m	H error, %
2	$\approx 765\ 000$	$\approx 310$	4,92	$\approx 0,4$
5	$\approx 330\ 000$	$\approx 140$	4,95	$\approx 1$
7	$\approx 105\ 000$	$\approx 50$	4,78	$\approx 4$

After analyzing the results, a base size of 5 mm was chosen, which is optimal for this flow part in time and accuracy of calculation. For generating the mesh, the following mesh models were selected:

- Polyhedral mesher;
- Surface remesher;
- Prizm layer mesher.

Parameters of generated mesh are presented are shown in Table 2:

**Table 2.** Parameters of generated mesh

Parameter	Value
Base size	5 mm
Prismatic Streching	1,5
Prismatic layer thickness, relative to the base size	25%
Number of prismatic layers	5

In the impeller and the pump diffuser, the mesh was reduced in 2 times to minimize the calculation error. An outlet pipe was also completed to stabilize the flow at the outlet of the pump diffuser and an inlet pipe to set the initial conditions. The resulting mesh in the cross section of the flow part is shown in Fig. 4.

To calculate the pressure and hydraulic efficiency at different values of gas content were selected physical models and were created 2 phases: gas (air) and liquid (water). Next, the “water-air” phase interaction was created and interaction models were selected.

As the boundary conditions at the inlet boundary, a constant mass flow rate was set corresponding to the flow at the optimal operation mode of the pump, at the outlet boundary constant pressure = 0 Pa was set.

In the initial conditions, only the gas content at the pump inlet was set and changed. The first 2 calculations were carried out at 0%, 1% gas, then the gas content at the inlet increased with step of 2% at first, then as the pressure and efficiency decreased with step of 1% to a permissible gas content.

With permissible gas content the head or hydraulic efficiency decreased in 2 times on a test bench or during the exploitation. To compare the obtained dependence of head on gas content the values of head were also obtained at a gas content of 9, 10, and 11%.

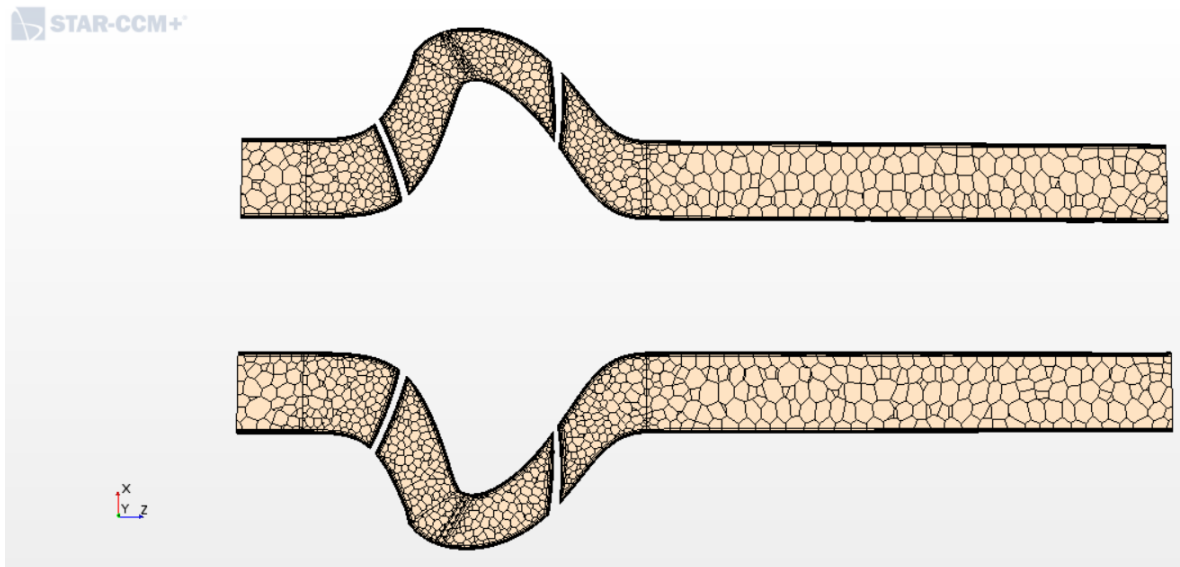


**Fig.4.** Resulting mesh in the cross section of the flow part

## Results

The modeling included  $\approx 20\,000$  iterations for each gas content for which stabilization of the flow occurred, which made it possible to obtain the correct values of head and hydraulic efficiency. Examples of multiphase flows modeling are given in articles [13-14]. The results of computational fluid dynamics modeling are presented in the form of Table 3:

**Table 3.** The results of computational fluid dynamics modeling

Gas content, %	H, m	$\eta_h$ , %
0	4,95	76,9
1	4,88	76,6
3	4,76	75,6
5	4,48	71,5
6	3,86	61,7
7	2,45	32,5
8	1,65	5,6

Also, basing on the obtained result, dependences of head and hydraulic efficiency on gas content at the inlet were plotted — Fig. 5, 6, respectively.

To verify the obtained modeling results, the dependence of head on gas content at the inlet was dimensionless and superimposed on the graph of head on gas content obtained experimentally by American scientists from Tulsa University, Oklahoma, USA [15–16]. Superimposed experimental and obtained dependences of head on gas content are presented in Fig. 7.

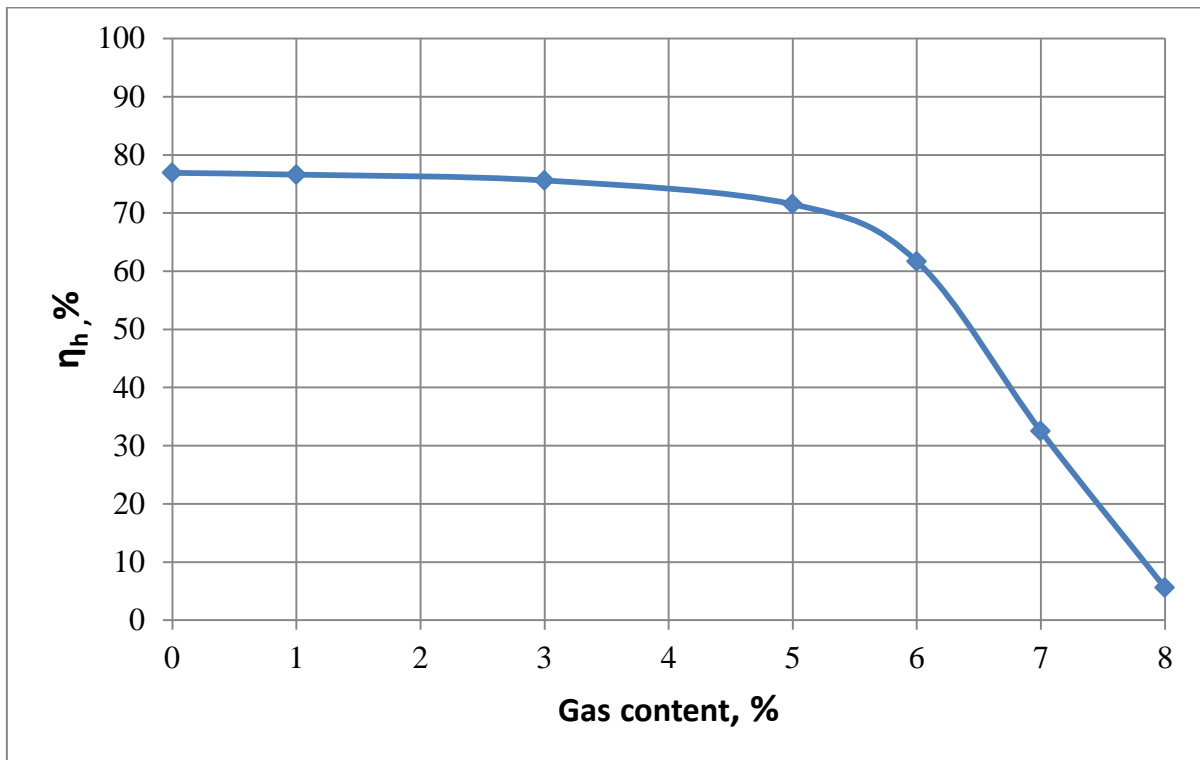


Fig.5. Dependence of hydraulic efficiency on gas content at the inlet

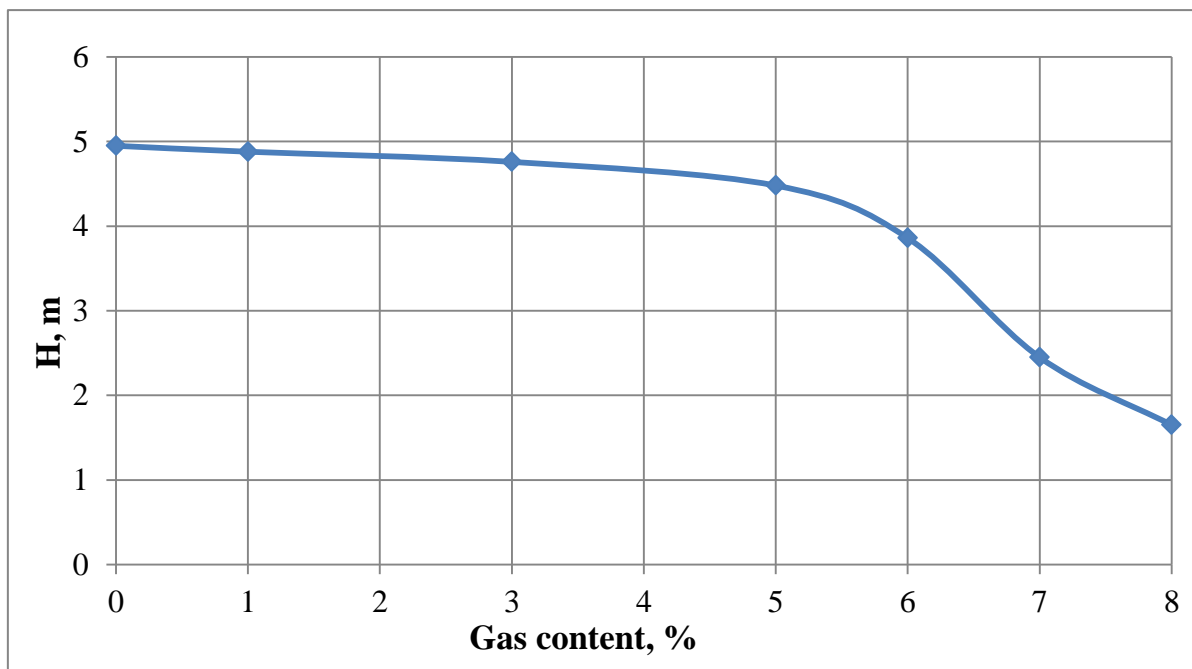


Fig.6. Dependence of head on gas content at the inlet

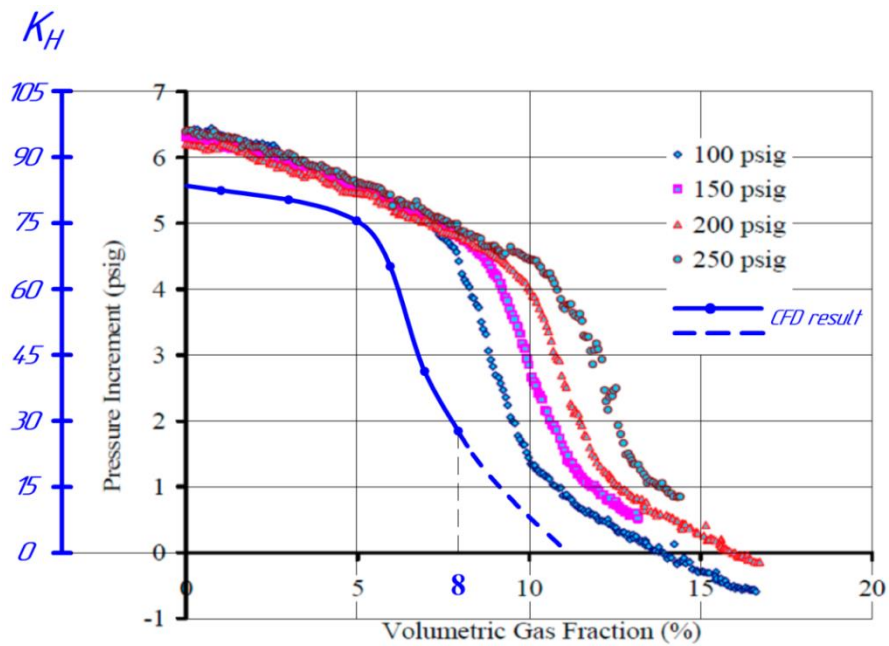


Fig.7. Superimposed experimental and obtained dependences of head on gas content are presented

$$K_H = \frac{H}{n^2 \cdot D_2^2} \cdot 10^{-6}$$

— dimensionless pressure coefficient,  $D_2$  — is the outlet diameter of the

impeller (m),  $n$  — is the set pump shaft rotational speed (rpm). The part of the dependency graph after 8% gas content is highlighted separately, since obtaining the average head for a gas content more than permissible there are some difficulties associated with the developed process of cavitation. Some difference in the value of the head coefficient from the experimental data is explained by the difference in the delivery coefficient of pumps.

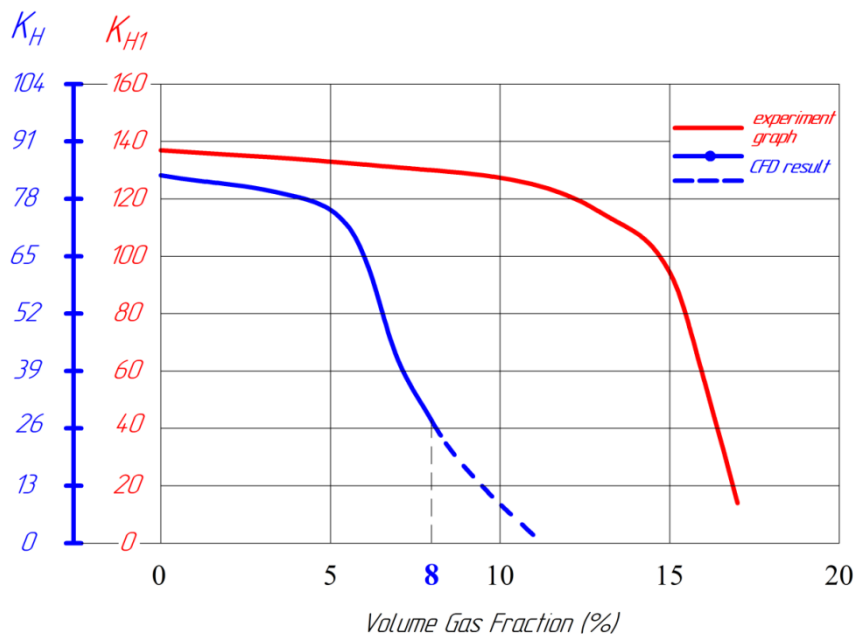


Fig. 8. Superimposed recalculated experimental dependence and dependence obtained by CFD methods

The obtained results can be superimposed on the experimental graphs obtained in the laboratory of the Gubkin Russian State University of Oil and Gas. The characteristic of the pump on the water-gas mixture was recalculated to the optimal operation mode of the pump under test; the head was dimensionless. To verify the results obtained by computational fluid dynamics modeling, Fig. 8 shows superimposed recalculated experimental dependence and dependence obtained by CFD methods.

$$K_{H1} = \frac{H}{n^2 \cdot D_2^2} \cdot 10^{-6} \text{ — dimensionless pressure coefficient, } D_2 \text{ — is the outlet diameter of the}$$

impeller of the pump under test (m),  $n$  — is the set pump shaft rotational speed (rpm).

It should be noted that the calculation was carried out at the designed pump stage, which was not optimized according to the criterion of increasing the permissible gas content. Therefore, this pump has a significantly smaller permissible present of gas for stable operation, what can be noticed on the graphs of comparison with existing pump stages. In the future, it is supposed to carry out such optimization by computational fluid dynamics modeling.

### Discussion

From Figures 7 and 8 show that the obtained dependence of head on gas content at the inlet is in good agreement with the graphs obtained experimentally, which confirms the adequacy of the mathematical model in the CFD software packages STAR CCM +.

Apparently, for designed pump stage, we can assume that the critical gas content at which the pressure and hydraulic efficiency are reduced by more than 2 times in comparison with the optimal operating mode is 7%. Good convergence of the computational fluid dynamics modeling results with experiment graphs means that to obtain a critical gas content it is not necessary to manufacture a pump or even pump stage, but rather to design a 3-D model of the flow part of one stage and to carry out a virtual experiment using computational fluid dynamics methods, which can significantly save the time on designing, optimization and manufacturing of the pump flow part.

Evaluation of the ability of a pump to operate on a multiphase flow using computational fluid dynamics method can be carried out from any sufficiently powerful computer with installed CFD software package (for example, ANSYS or STAR CCM +) in a matter of days. Besides, the hydrodynamic modeling does not require the manufacture of a test bench, which significantly saves time and money on its design and manufacture.

When doing geological and geophysical exploration on a well, the percentage of associated gas in oil is pretty important indicator, which depends on depth of oil occurrence, the configuration and location of the oil formation, and other factors. In wells with associated gas content less than critical, it is possible to install a pump for pumping the oil-associated gas mixture, and then there is no need to install additional modules at the pump inlet, which significantly saves financial costs for the purchase of pump equipment and reduces its dimensions.

Thus, the value of the critical or permissible gas content is a very important indicator during the designing of the flow part of the pump, in calculating the cost of ESP installation for oil production and in calculating the economic indicators of production.

### List of reference

- [1] Barrios Castellanos, M., Serpa, A.L., Biazussi, J.L., Monte Verde, W., do Socorro Dias Arrifano Sassim, N. Fault identification using a chain of decision trees in an electrical submersible pump operating in a liquid-gas flow (2020) *Journal of Petroleum Science and Engineering*, 184, article № 106490.
- [2] Curkan, B., Klaczek, W., Reede, C. High temperature ESPs for geothermal production: The ideal pump (2018) *Transactions — Geothermal Resources Council*, 42, pp. 1894–1908.
- [3] Wang, Q., Liu, Y., Yang, J., Cui, M., Qi, D. A novel downhole gas separator in ESP systems (2018) *Society of Petroleum Engineers — SPE Asia Pacific Oil and Gas Conference and Exhibition 2018, APOGCE 2018*.

- [4] Camilleri, L., El Gindy, M., Rusakov, A., Ginawi, I., Abdelmotaal, H., Sayed, E., Edris, T., Karam, M. Increasing production with high-frequency and high-resolution flow rate measurements from ESPs (2017) Society of Petroleum Engineers — SPE Electric Submersible Pump Symposium 2017, pp.
- [5] Boyarshinova, A., Lomakin, V., Petrov, A. Comparison of various simulation methods of a two-phase flow in a multiphase pump (2019) IOP Conference Series: Materials Science and Engineering, 589 (1), article № 012014.
- [6] Lomakin, V.O., Kuleshova, M.S., Kraeva, E.A. Fluid Flow in the Throttle Channel in the Presence of Cavitation (2015) Procedia Engineering, 106, pp. 27–35.
- [7] Lomakin, V., Cheremushkin, V., Chaburko, P. Investigation of vortex and hysteresis effects in the inlet device of a centrifugal pump (2018) 2018 Global Fluid Power Society PhD Symposium, GFPS 2018, article № 8472374.
- [8] Petrov, A., Isaev, N., Kuleshova, M. Test bench flow straightener design investigation and optimization with computational fluid dynamics methods (2019) IOP Conference Series: Materials Science and Engineering, 492 (1), article № 012036.
- [9] Tkachuk, V., Navas, H., Petrov, A., Protopopov, A. Hydrodynamic modelling of the impact of viscosity on the characteristics of a centrifugal pump (2019) IOP Conference Series: Materials Science and Engineering, 589 (1), article № 012007.
- [10] Budaev, G., Danilov, D., Kuznechov, A., Lomakin, V., Cheremushkin, V. Research of centrifugal gas-liquid separator (2019) IOP Conference Series: Materials Science and Engineering, 589 (1), article № 012035.
- [11] Saprykina, M., Lomakin, V. The evaluation of the effect of gas content on the characteristics of a Centrifugal Pump (2019) IOP Conference Series: Materials Science and Engineering, 589 (1), article № 012017.
- [12] Petrov, A., Morozov, A., Kuleshova, M. Investigation of hermetic low-speed pumps performance when operating on highly viscous liquids (2019) IOP Conference Series: Materials Science and Engineering, 589 (1), article № 012030.
- [13] Tarodiya, R., Gandhi, B.K. Numerical simulation of a centrifugal slurry pump handling solid-liquid mixture: Effect of solids on flow field and performance (2019) Advanced Powder Technology, 30 (10), pp. 2225–2239.
- [14] Olive, N.R., Hong-Quan-Zhang, Redus, C.L., Brill, J.P. Experimental study of low liquid loading gas-liquid flow in near-horizontal pipes (2001) Proceedings of the Engineering Technology Conference on Energy, B, pp. 777–782.
- [15] Zhang, H.-Q.; Wang, Q.; Sarica, C.; Brill, J.P. Unified model for gas-liquid pipe flow via slug dynamics—Part 2: Model validation. *J. Energy Resour. Technol.* 2003, 125, 274–283.
- [16] Zhu, J.; Zhang, H.-Q. A Review of Experiments and Modeling of Gas-Liquid Flow in Electrical Submersible Pumps. *Energies* 2018, 11, 180.